Sensors and Actuators Reports 4 (2022) 100073

Contents lists available at ScienceDirect

Sensors and Actuators Reports

journal homepage: www.sciencedirect.com/journal/sensors-and-actuators-reports

Electrochemical sensor for isoniazid detection by using a WS_2/CNTs nanocomposite

Berlane G. Santos [a], Josué M. Gonçalves [a], Diego P. Rocha [a,e], Giane S. Higino [b], Thakur P. Yadav [c], Jairo J. Pedrotti [b], Pulickel M. Ajayan [d], Lucio Angnes [a,*]

[a] Department of Fundamental Chemistry, Institute of Chemistry, University of São Paulo, Prof. Lineu Prestes Avenue, 748, 05508-000 São Paulo, SP, Brazil
[b] Engineering School - Mackenzie Presbyterian University, Rua da Consolação, 896, 01302-907 São Paulo, SP, Brazil
[c] Department of Physics, Institute of Science, Banaras Hindu University, Varanasi 221005, India
[d] Department of Materials Science and NanoEngineering Rice University, 6100 Main St, Houston, TX 77005 United States
[e] Federal Institute of Paraná (IFPR), Rua José de Alencar, 1080, 85200000, Pitanga, PR, Brazil

ARTICLE INFO

Keywords:
Electrochemical sensor
Carbon nanotubes
Composites
Isoniazid

ABSTRACT

This paper presents a new modified electrode that combines the high electrical conductivity of carbon nanotubes (CNTs) with the catalytic sites of WS_2 (named WS_2/CNTs) for isoniazid detection. Electrochemical and electroanalytical properties of the WS_2/CNTs/glassy carbon electrode (GCE)-modified electrodes were investigated by cyclic voltammetry and differential pulse voltammetry (DPV). The composite material was characterized by Raman spectroscopy, X-ray diffractometry (XRD), and scanning electron microscopy . The electrochemical performance of the WS_2/CNTs/GCE sensor exhibited a limit of detection of 0.24 μM with a linear range from 10 to 80 μM of isoniazid using DPV. This sensor provided enhanced stability and electrocatalytic activity for isoniazid oxidation reactions. Recoveries ranging from 96.9 to 104.5% were calculated, demonstrating satisfactory accuracy of the proposed method. The improvement of electrochemical activity was assigned to synergic effects obtained by combining the catalytic sites from WS_2 and the known electrical conductivity and large surface area of the CNTs, resulting in an anticipation of the oxidation peak of isoniazid in about 400 mV in comparison with bare GCE.

1. Introduction

Isoniazid (isonicotinic acid hydrazide or pyridine-4-carboxylic acid hydrazide) is a widely prescribed antibiotic drug for treating tuberculosis [1], one of the top ten causes of human death, afflicting approximately 10 million people every year [2]. It is supposed that isoniazid has a toxic effect on the liver and can increase the rate of hepatotoxicity when co-administered with rifampicin [3]. An overdose of this drug can cause seizures, metabolic acidosis, coma, and even death [4]. In that sense, rapid and precise control of plasma levels for this drug is highly desirable. Many approaches have been applied to detect isoniazid, including colorimetry [5], fluorimetry [6], titrimetry [7], chromatography [8], indirect atomic absorption spectrometry [9], liquid chromatography-mass spectrometry [10] and derivative spectrophotometry [11]. Although these methods have their advantages, they are generally most laborious and require time-consuming sample processing. Additionally, they lack portability and, in some cases, demand multifaceted pretreatment by high pure solvent or reagents [2,4,12].

Considering the isoniazid clinical relevance, developing low-cost, simple, and selective analytical methods is crucial for fast detection in low concentrations in biological fluids and pharmaceutical formulations. Electrochemical sensing is an attractive alternative in drug quantification thanks to operational simplicity, speediness, good selectivity, high sensitivity, low volume consumption, and real-time nature [2]. In fact, electrochemical methods have integral benefits over other well-established analytical procedures [13]. In addition, the development of electrodes modified with nanomaterials and nanocomposites for electroanalytical purposes is a tendency that is gaining increasing applications thanks to the large surface area, excellent electrical conductivity, good chemical and mechanical stability. Electrocatalytic properties can be tailor-made, proportioning electrochemical sensors with an enhanced analytical response and sensitivity [14].

Recently, papers reported the use of nanomaterials in the electrochemical detection of isoniazid [4,15,16]. However, in a recent study

* Corresponding author.
E-mail addresses: jairo.pedrotti@mackenzie.br (J.J. Pedrotti), luangnes@iq.usp.br (L. Angnes).

https://doi.org/10.1016/j.snr.2021.100073
Received 19 October 2021; Received in revised form 10 December 2021; Accepted 20 December 2021
Available online 2 January 2022

reported by R. Chokkareddy & G. G. Redhi [13], is established "there is still requirement to search for novel nanocomposites providing high sensitivity, low oxidation, low limit of detection (LOD) and quick electron transfer kinetics for isoniazid detection".

Among the nanomaterials/nanocomposites used as electrochemical sensors in detecting and quantifying isoniazid, it is possible to mention those based on nanocarbons, nanoparticles, and composite materials. For instance, Shahrokhian and Amiri [17] reported the design and preparation of the carbon-paste electrodes modified with multiwalled carbon nanotubes (MWNTs). The linear range was 1 μM – 1 mM for isoniazid and the detection limit was 0.5 μM. Spindola *et al.* [18], built up a sensor for analysis of isoniazid applying graphene-functionalized MWNTs as support for iron phthalocyanine on glassy carbon electrode (GCE), forming FePc/f-MWCNT/GC electrode (FePc/f-MWCNT). Under optimized conditions, a linear response range from 5 to 476 μM was obtained with an LOD and sensitivity of 0.56 μM and 0.023 μA L μM^{-1}, respectively, demonstrating the potential of the new sensor.

As mentioned earlier, monitoring isoniazid by nanoparticles-based sensors as an active site is also a widely used strategy, especially those containing transition metals. For example, Oliveira *et al.* [19] developed a rapid and simple method for amperometric isoniazid determination by flow injection analysis (FIA) using a screen-printed carbon electrode (SPCE) modified with silver hexacyanoferrate (NPAg-HCF). The catalytic response of the SPCE/NPAg-HCF electrode for isoniazid showed a linear concentration range from 5.0 μM to 0.5 mM and LOD of 2.6 μM.

In another study, Absalan and collaborators [20] reported the preparation of 30–100 nm palladium nanoparticles by electrodeposition on a carbon ionic liquid electrode (PdNPs/CILE). This electrode proportionated excellent electrocatalysis for oxidation of isoniazid at pH = 7.0 and 0.34 V *vs.* Ag/AgCl operating potential. By cyclic voltammetry (CV) measurements, linear ranges between 5.0 μM – 100 μM and 0.15 mM – 2.6 mM isoniazid and a low LOD of 0.47 μM were determined. The present study describes the development of a GCE modified with a composite material, combining the high electrical conductivity of carbon nanotubes (CNTs) with the catalytic sites of WS_2.

WS_2 is a transition metal dichalcogenide composed of a layer of tungsten sandwiched in two layers of sulfur and stacked by weak Van der Waals interactions [21]. It has good dispersibility in water, good biocompatibility and large electroactive surface area [22, 23]. As a semiconductor, WS_2 alone does not have good applicability as an electrode modifier due to its low conductivity, so it is highly desirable to prepare WS_2 in a conductive support to improve charge transfer processes and application as an electrochemical sensor [24]. Therefore, combining WS_2 with CNTs to prepare a nanocomposite is a good way to overcome the low conductivity of WS_2.

The proposed sensor presented enhanced stability and electrocatalytic activity for isoniazid oxidation reactions. Electrochemical and electroanalytical properties of the WS_2/CNTs/GC-modified electrode were investigated by CV and differential pulse voltammetry (DPV). The composite material was characterized by Raman spectroscopy, X-ray diffractometry (XRD) and scanning electron microscopy (SEM).

2. Materials and methods

2.1. Chemicals, materials, and samples

All chemicals utilized were of analytical grade and were used without further purification. Benzene, ferrocene, WS_2 powder, urea, glucose, uric acid, hexaammineruthenium (III) chloride and carbon nanotubes were purchased from Sigma Aldrich (St. Louis, USA). Sodium chloride, potassium chloride, sodium sulfate, potassium dihydrogen phosphate were obtained from Synth (Diadema, Brazil). Isoniazid, hydroquinone, calcium chloride dihydrate, ammonium chloride, and ascorbic acid were acquired from Merck (Darmstadt, Germany). Potassium ferricyanide and potassium ferrocyanide were purchased from CAAL (São Paulo, Brazil) and Carlo Erba (Barcelona, Spain), respectively. Perchloric acid was obtained from Vetec (Rio de Janeiro, Brazil). Solutions were prepared daily by dissolving or diluting appropriate amounts of the reagents in water or in a suitable background electrolyte, utilizing water from a Millipore Milli-Q system (resistivity ≥ 18.2 MΩ cm). Synthetic urine sample was prepared as described by Silva *et al.* [25]. For this purpose, 0.73 g NaCl, 0.40 g KCl, 0.27 g $CaCl_2 \bullet 2H_2O$, 0.56 g Na_2SO_4, 0.35 g KH_2PO_4, 0.25 g NH_4Cl, and 6.25 g urea were placed in a 250 mL volumetric flask, which was completed with high purity deionized water. The urine sample was doped with 10 μM of isoniazid, and the final solution was analyzed.

2.2. Preparation of the WS_2/CNTs

The carbon nanotubes (CNTs) were acquired from Aldrich and used without any additional treatment. The two-dimensional (2D) tungsten disulfide (WS_2) was synthesized using bulk WS_2 powder by ultrasound-assisted liquid phase exfoliation in n-methyl-2-pyrrolidone (NMP) solvent. The WS_2 was dispersed in NMP solvent with 2 mg mL^{-1} concentration and subsequently exfoliated using ultrasound for 4 h. The sonication was carried out in an ice-cooled water bath system keeping the temperature below to 10 °C. The solution containing the dispersed WS_2—NMP was transferred to a centrifuge to separate the bulk aggregates at 5000 rpm. The supernatant liquid (from the centrifuged solution) was collected carefully and transferred to a flask, which was completed to 200 mL with deionized water. In sequence, 100 mg of CNTs was added to 200 mL WS_2-deionized water solution and stirred for 30 min. Further, WS_2-deionized water-CNT mixed solution was exfoliated for one more hour. The obtained solution was filtered using a 0.22 μm microporous membrane, and subsequently, the solid portion was washed with deionized water several times and dried at 80 °C for 12 h for applications.

2.3. Preparation of the WS_2/CNTs/GC modified electrode

5 mg of WS_2/CNTs was added in 5 mL of ethanol and this solution was sonicated for 30 min to form a suspension. A volume of 5 μL of this suspension was drop-casted onto a polished glassy carbon electrode and the ethanol was evaporated using a mild heat from a heat blower. This procedure was done twice. **Scheme 1** illustrates the process.

2.4. Electrochemical measurements

All electrochemical measurements (cyclic voltammetry - CV and differential pulse voltammetry - DPV) were carried out in a three-electrode standard cell coupled to a PGSTAT128N potentiostat/galvanostat from Autolab (Eco Chemie, Utrecht, The Netherlands) controlled by a laptop running NOVA 2.1.3 software. Cyclic voltammetric measurements were carried out using standard solutions containing 1.0 mM of ferri/ferrocyanide redox couple, hexaammineruthenium (III) chloride, hydroquinone, and isoniazid, in supporting electrolyte 0.1 M KCl, except for hydroquinone ($HClO_4$ 0.1 M). CV conditions: scan rate of 100 mV s^{-1} and step potential of 5 mV. DPV was used to register calibrations curves for this drug after optimizing parameters (modulation amplitude 60 mV, step potential 6 mV, and modulation time 60 ms). Baseline-correction was applied for all DPV data for better viewing of the peaks and the treatment was performed using the "moving average" algorithm, with window size set to 2, available in the software NOVA (version 2.1.3). All experiments were carried out at laboratory temperature (25 ± 2 °C) without oxygen removal. An Ag/AgCl/KCl_{sat}, a platinum wire, and a pristine and modified glassy carbon ($\varnothing$ = 3 mm) were used as reference, counter, and working electrodes, respectively. Electrochemical impedance spectroscopic (EIS) measurements were acquired from a PGSTAT 128 N potentiostat/galvanostat containing the FRA2 module controlled by a laptop running NOVA 1.11.0 software, which was also used for data acquisition.

2.5. Characterization

WS_2/CNT were characterized by Raman spectroscopy using a Witec 300R Alpha confocal spectrometer (Germany) equipped with objective lens (Olympus) with 20x magnification, 532 nm Ar laser, and the power and integration time set to 0.37 mW and 8 s. The scanning electron microscopy (SEM) images were registered using a JEOL JSM-7401F microscope (Jeol Ltd, Tokyo, Japan), with the samples prepared on copper supports using carbon tape. Elemental mapping was recorded by energy-dispersive X-ray spectroscopy (EDS) using a 20 mm^2 silicon drift detector (SDD). The composite was also characterized by X-ray diffractometry (XRD) in a Bruker D2 Phaser equipment (Germany) with a Cu Kα source (λ = 1.5418 Å, 30 kV, 15 mA, step = 0.05°) in the 2θ range from 5 to 80°.

3. Results and discussion

3.1. Physical and chemical characterizations of the WS_2/CNTs

The SEM images of WS_2/CNT depict microplates of WS_2 interconnected by CNTs network, which were acting as conducting wires and turning the composite electrically connected [26] (**Fig. 1A-1B**). In fact, the WS_2/CNT heterogeneous composites can be characterized as layered WS_2 microplates of various sizes and thicknesses in the range of a few wrapped with CNTs. The chemical analysis of the WS_2/CNT composites enabled by SEM-EDS elemental mapping typical results are shown in **Fig. 1D-1F**. As expected, it can be clearly seen by comparing the elemental mappings that there is a correlation between the position of W and S in some regions of the image, it corresponds exactly to WS_2 positions in the electronic image, while the presence of carbon is more distributed throughout the composite, which are consistent with the SEM observations depicted in **Fig. 1C**.

The XRD of powdered WS_2/CNT composites (**Fig. 2A**) exhibited a predominant diffraction peak at 2θ = 14.43° (6.18 Å), typical of the (002) reflection planes of WS_2, indicating the predominance of these crystal planes in the sample [27,28]. Other minor diffractions peaks from (004), (100), (101), (103), (006), (105), (106), (008), (112), (114), (200), (203) and (216) planes were also observed, matching with highly crystalline hexagonal structure (JCPDS 08–0237, P63/ mmc space group, 2H-WS_2) [27,28]. On the other hand, it was not possible to obtain information from CNTs by XRD, possibly due to their low crystallinity.

Additional information related to the presence of CNTs was obtained by Raman spectroscopy. As shown in **Fig. 2B**, peaks at 1335 cm^{-1} and 1580 cm^{-1} are well-defined for the D and G band respectively in the Raman spectra of WS_2/CNT composite. It is to be noted that the sp^3 disordered carbon is represented by the D band and the sp^2 graphitic carbon is represented by the G band [29]. In addition, the Raman spectrum shows other bands that are attributed to the presence of WS_2 in the composite material [30,31], confirming the presence of both materials in the hybrid constitution.

3.2. Electrochemical characterization

To evaluate the performance of the modified WS_2/CNT electrodes cyclic voltammetry was the technique chosen. The first experiments involved the reversible couple ferri/ferrocyanide, hexaammineruthenium (III) chloride, hydroquinone and isoniazid. The typical results are presented in **Fig. 3**.

According to the figure, it is possible to see that there was a significant difference in electrochemical behavior for all evaluated analytes regarding peak current (I_p), peak definition, and peak-to-peak separation (ΔE_p), comparing the bare and the modified electrode. In the case of the ferro/ferricyanide analysis (**Fig. 3A**), the bare GC electrode provided lower I_p when compared to the modified surface. For instance, the response of the glassy carbon electrode (GCE) after the modification with WS_2/CNT increased around 2-fold in both I_{pa} and I_{pc}. No major changes in ΔE_p for hexaammineruthenium (III) chloride was observed (**Fig. 3B**), however an increase around four times in current was achieved. Significant changes were acquired for the electrochemical behavior of the hydroquinone (**Fig. 3C**), being able to notice that the modification of the GCE was able to provide an increase in the anodic current around 5 times, a significant reduction in the ΔE_p and in addition to well-defined and sharp peaks. Regarding isoniazid detection (**Fig. 3D**), it is possible to note that the bare surface provides a low-intensity electrochemical signal. On the other hand, on the modified electrode, a well-defined peak around 0.45 V was acquired. **Table 1** summarizes the data obtained from **Fig. 3** regarding peak potential (E_p), I_p, and ΔE_p before (BM) and after (AM) electrode modification. Thus, based on the aforementioned, it is possible to conclude that the GCE modification with the WS_2/CNT favored the electron transfer processes

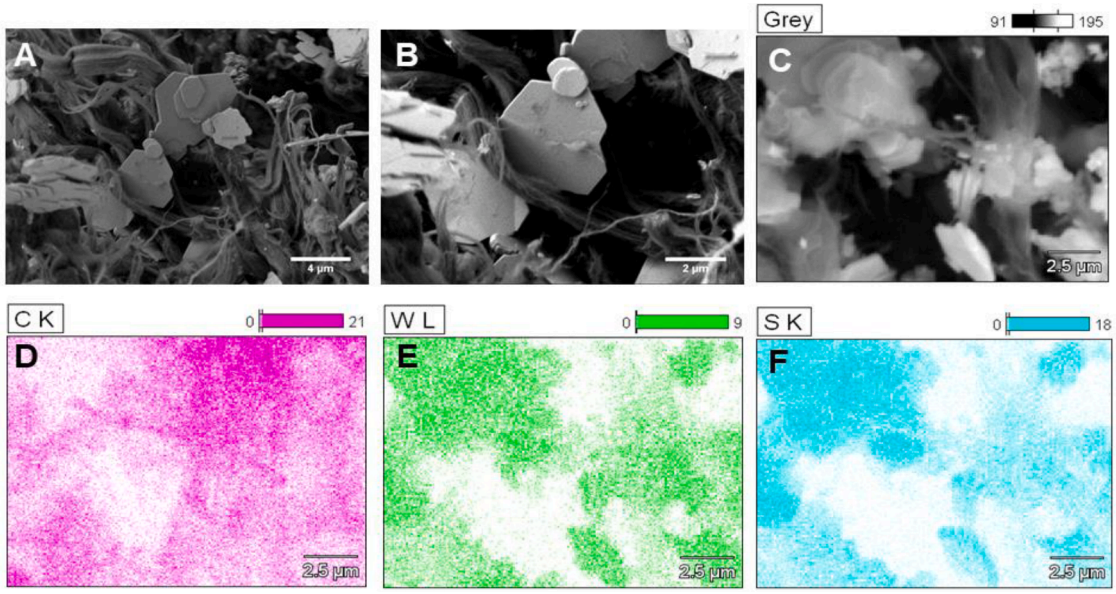

Fig. 1. (A-B) SEM images of WS_2/CNT composites. The images magnifications increase from left to right, 5000 x (A), and 10,000 x (B and C), respectively. EDS elemental mapping of the WS_2/CNT composites: (C) SEM image and corresponding elemental mapping of (D) carbon, (E) tungsten and (F) sulfur.

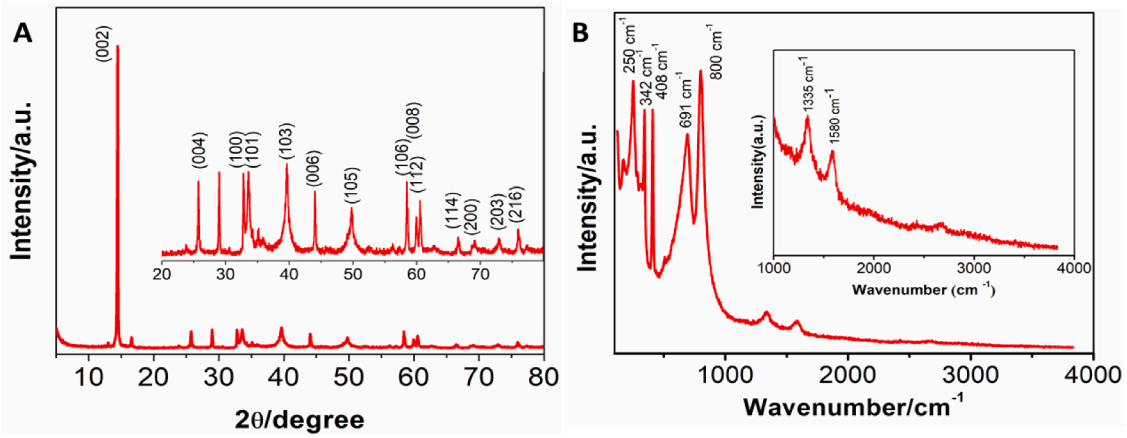

Fig. 2. (A) X-ray diffractograms and (B) Raman spectrum of WS_2/CNT composite powder. In Fig. 2(A) the peaks situated between 20 and 80° were enlarged for clarity. In Fig. 2(B), the region from 1000 to 4000 was enhanced to show clearly the peaks corresponding to the D and G bands of the CNTs.

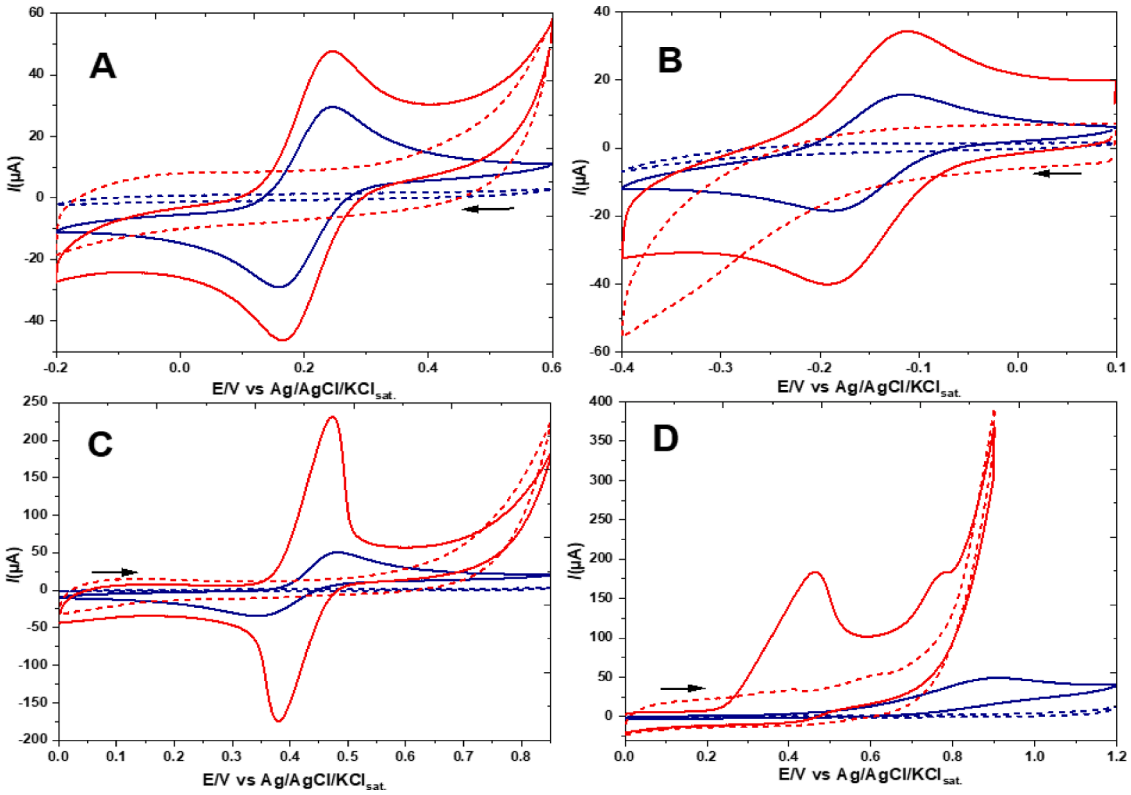

Fig. 3. Cyclic voltammetric recordings in the presence (1.0 mM) (solid lines) and absence (dashed lines) of (A) ferri/ferrocyanide redox couple, (B) hexaammineruthenium (III) chloride, (C) hydroquinone, and (D) isoniazid, before (blue line) and after (red lines) GCE modification. Supporting electrolyte: 0.1 M KCl, except for hydroquinone ($HClO_4$ 0.1 M). CV conditions: scan rate of 100 mV s^{-1} and step potential of 5 mV.

Table 1
Data obtained from Fig. 3 regarding E_p, I_p, and ΔE_p before (BM) and after (AM) modification of the GC electrode with WS_2/CNT.

Analyte		E_{pa} (V)	E_{pc} (V)	I_{pa} (μA)	I_{pc} (μA)	ΔE_p (V)
$[Fe(CN)_6]^{3-/4-}$	BM	0.24	0.15	29.5	−46.6	0.09
	AM	0.24	0.16	49.7	−29.0	0.08
$[Ru(NH_3)_6]^{3+}$	BM	−0.11	−0.18	15.8	−18.4	0.07
	AM	−0.11	−0.19	34.4	−40.1	0.08
Hydroquinone	BM	0.48	0.34	50.48	−34.5	0.14
	AM	0.47	0.38	230.4	−175.0	0.09
Isoniazid	BM	0.91	–	49.4	–	–
	AM	0.46	–	184.0	–	–

enhancing its electrochemical performance. The improvement of electrochemical activity can be directly attributed to its large surface area, high electron conductivity, and synergic effects obtained by combining the catalytic sites from WS_2 and the known electrical conductivity of the CNTs [32].

In addition, EIS measurements were used to evaluate the charge transfer resistance (R_{CT}) in both GCE and WS_2/CNT/CGE in 1.0 mM $[Fe(CN)_6]^{3-/4-}$ solution, using 0.1 mol L^{-1} KCl solution as supporting electrolyte. Fig. 4**A** shows the Nyquist plots (and respective fits) and equivalent circuits of bare GCE (Fig. 4**B**) and WS_2/CNT modified CGE (Fig. 4**C**). The Nyquist plot for bare GCE shows a semicircle in the high-frequency region and an inclined straight line in the low-frequency

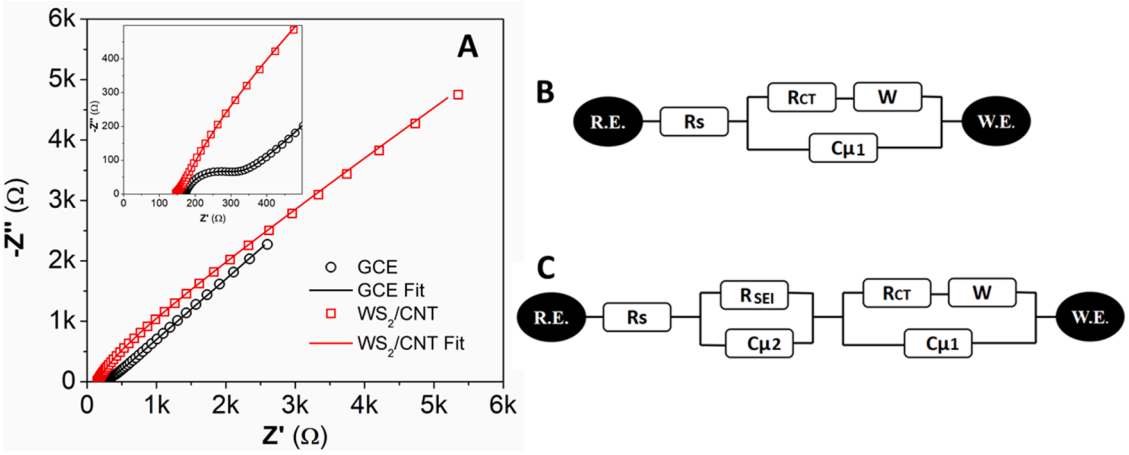

Fig. 4. (A) Nyquist plot of GCE and WS_2/CNT/CGE. The EIS measurements were carried out in 1.0 m M $[Fe(CN)_6]^{3-/4-}$ solution in 0.1 M KCl solution at OCP potential, and superimposed AC signal with 10 mV, in the 0.01 to 10,000 Hz range. R_S = electrolyte resistance, R_{CT} = charge transfer resistance, R_{SEI} = solid electrode interphase resistance, $C_{\mu 1}$ = constant phase elements, $C_{\mu 1}$ = constant phase elements that represent the double-layer capacitor, Z_w stands for the diffusion resistance.

region, characterized by a Randles circuit with a charge transfer resistance (R_{CT}) value of 140 Ω. On the other hand, the WS_2/CNT/CGE shows a more complex equivalent circuit, containing other elements such as the R_{SEI} and Cμ2 attributed respectively to the solid electrode interphase resistance and the constant phase elements, as already reported for other composites containing WS_2 [33]. The R_{CT} (9 Ω) of WS_2/CNT/CGE is smaller than that of the bare GCE (R_{CT} = 140 Ω), indicating that WS_2/CNT can effectively enhance the electrode kinetics and electrocatalytic activity of GCE.

To evaluate the response of the modified electrode, a series of cyclic voltammograms was carried out increasing the scan rate in the range between 0.005 V s^{-1} and 0.2 V s^{-1} in the presence of 1.0 mM ferri/ferrocyanide redox couple (Fig. 5A) and 1.0 mM isoniazid (Fig. 5C). Fig. 5B and 5C display the relation of I_{pa} and I_{pc} *versus* the square root of scan rate ($v^{0.5}$) for ferri/ferrocyanide redox couple and isoniazid, respectively. In both cases, a linear response (R^2 = 0.999) was observed, indicating that the mass transport of the ferri/ferrocyanide redox couple and isoniazid was controlled by diffusion. Scheme 2 shows the mechanism for electrochemical oxidation of isoniazid. [34].

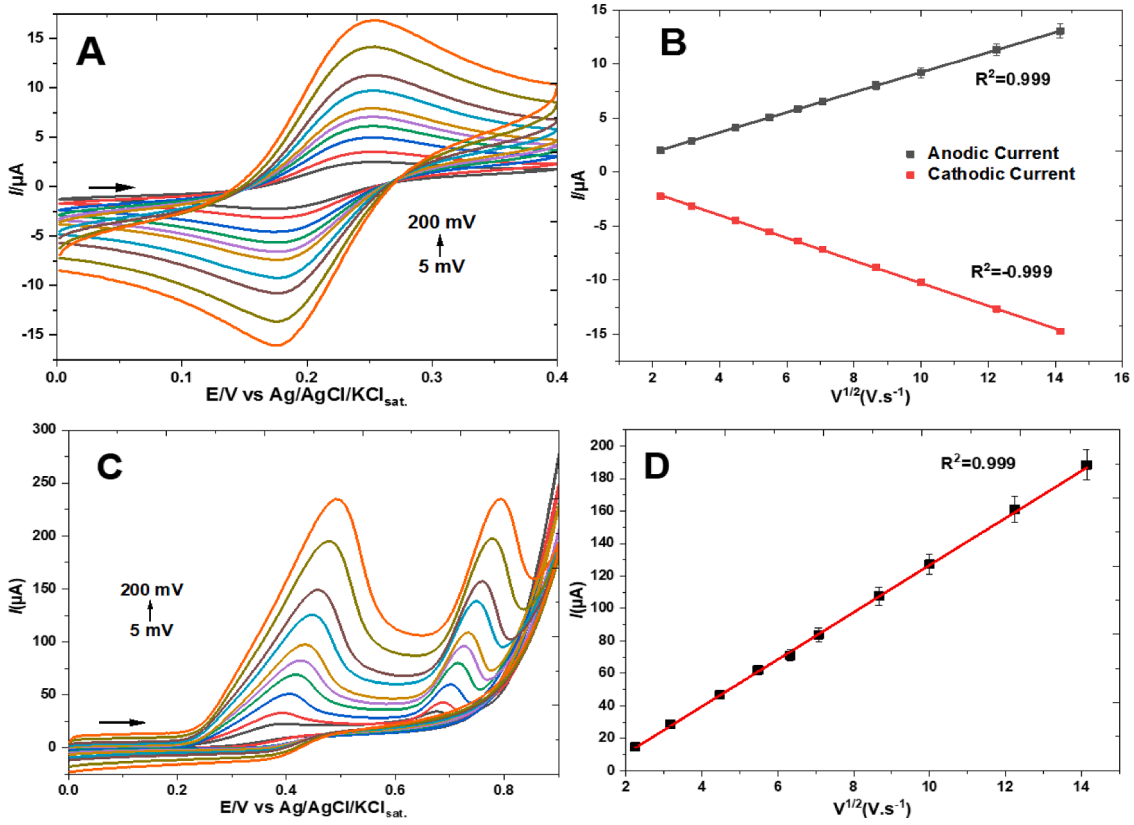

Fig. 5. Cyclic voltammograms recorded in the presence of 1.0 mM ferri/ferrocyanide redox couple (A) and in the presence of 1.0 mM isoniazid (C), both in 0.1 M KCl solution (background electrolyte) at different scan rates (5 to 200 mV s^{-1}). (B and D) Relation of anodic (■) and cathodic (■) peak currents *versus* the square root of the scan rate ($\upsilon^{0.5}$).

3.3. Optimization and analytical features

The proposed electrode was developed and applied in the sensing of isoniazid. Two different electrochemical techniques (square-wave voltammetry – SWV and differential-pulse voltammetry - DPV) were initially tested for this purpose. DPV technique showed to be highly promising for such detection, and its results will be shown in the sequence. Thus, in order to perform the analysis of low concentrations of isoniazid, the parameters that affect the DPV technique, such as modulation time, step potential and modulation amplitude, were carefully optimized towards the detection of 10 μM isoniazid. The effect of the step potential on the analytical signal was evaluated in the interval between 1 and 10 mVwhile the modulation amplitude and modulation time parameters were optimized in the range between 30 mV and 90 mV and 20 ms and 100 ms, respectively. Well-defined and sharp peaks, lower deviation, and higher peak currents were acquired when 6 mV, 60 mV, and 60 ms were used as step potential, modulation amplitude, and modulation time, respectively. Therefore, these values were selected for further experiments.

Under the optimized conditions, a linear response for isoniazid ranging from 10 μM to 80 μM with a coefficient of determination (R^2) of 0.990 was observed (Fig. 6**A**). The relation between peak current and the drug concentration can be described by the equation $Y = 0.91 + 0.33$ $C_{isoniazid}$ (μM) (Fig. 6**B**). Also to assess the repeatability and reproducibility of the modified electrode preparation, different measurements were taken with the same modification and with different modifications. Table 2 and 3 show the values obtained with the respective errors. For measurements with the same modification, a relative standard deviation (RSD) of 1.97% was calculated, which reflects a good repeatability, and for measurements with different modifications, the calculated RSD was 3.61%. The detection and quantification limits of the new isoniazid sensor were estimated respectively as 0.24 μM (99.7% confidence level) and 0.79 μM, following: $3S_b/m$ and $10S_b/m$ where S_b and m were the standard deviation for ten consecutive measurements of the baseline noise and the slope of the analytical curve, respectively [35]. Experimentally LOD values were determined by adding concentrations from 1.0 μM, it is noted that around 1.0 μM it is possible to verify the difference between the analyte signal and the noise. The proposed modified electrode provided excellent features (wide linear range and low detection limit) for the analyte determination, being able to monitor concentrations of this compound at trace levels.

After the evaluation of the analytical features, the developed method was employed for isoniazid determination in three samples of synthetic urine. The samples were diluted ten times in 0.10 M KCl (background electrolyte). Posteriorly, the samples were spiked with a low isoniazid concentration (10 μM). Satisfactory recoveries ranging from 96.9 to 104.5% were achieved, showing suitable accuracy of the method developed, especially taking into account the low concentration employed for the experiments. Standard addition curves provided good linearity ($R^2 > 0.99$) and the results are displayed in Fig. 6**C**-6**D**.

Table 4 provides an overview regarding different modified electrodes utilized for isoniazid analysis. The analysis of this table demonstrates that the developed sensor presented performance comparable and even better in comparison with others found in the literature regarding detection limit and linear range. For instance, the detection limit reached in the proposed protocol (0.24 μM) was 14- and 6-fold lower than that achieved by Aguirre-Araque et al. [1] and Liang and colleagues [36], respectively. On the other hand, Chokkareddy and coworkers [37] developed a composite electrode based on multiwalled carbon nanotubes, HRP, and TiO_2 nanoparticles, which attained LOD value of 0.0335 μM (7-fold lower than that estimated in this work); however, such electrodes achieved a lower linear range (between 0.5

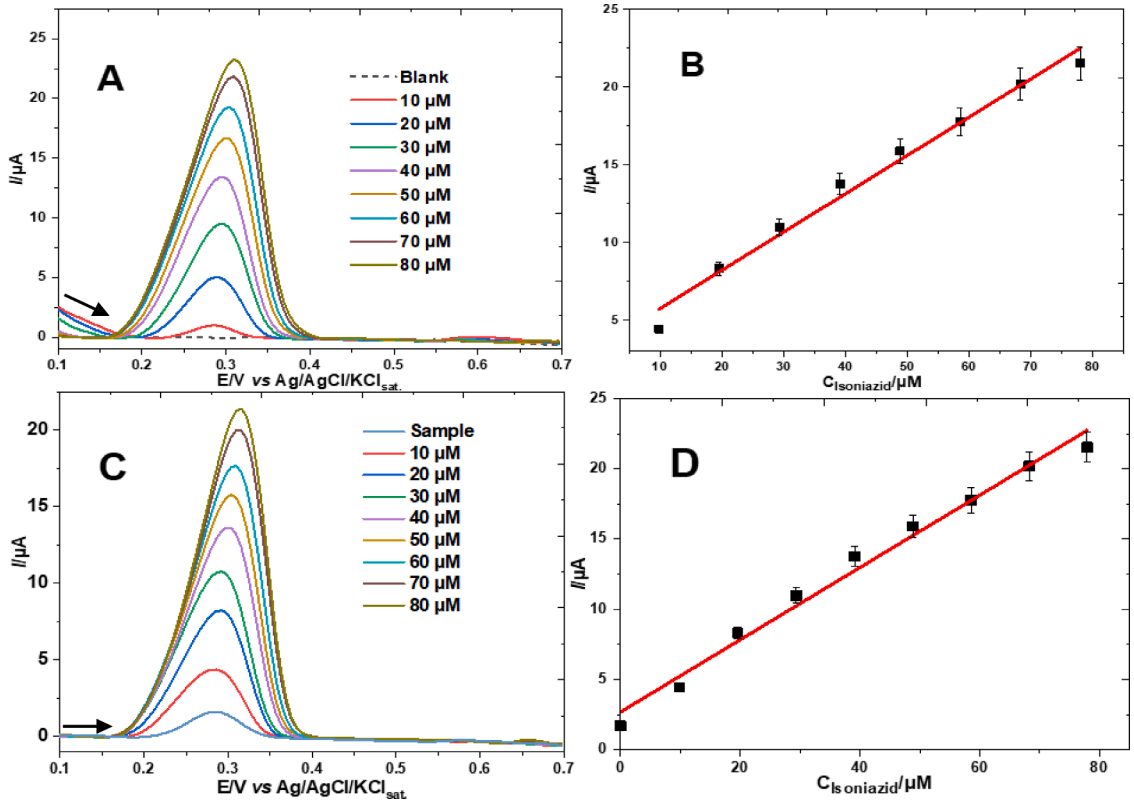

Fig. 6. (A) DPV recordings for increasing isoniazid concentrations (10 to 80 μM, injected on a pure electrolyte) and the following curves correspond to the concentrations indicated inside the figure, using the WS_2/CNT/GC electrode; (B) Respective analytical curve.; (C) Analysis of synthetic urine followed by injections of increasing concentrations (10 to 80 μM) of the analyte; (D) plot of peak current in function of isoniazid concentrations. Experimental conditions: DPV modulation amplitude: 60 mV; modulation time: 60 ms; step: 6 mV. Background electrolyte: 0.1 M KCl.

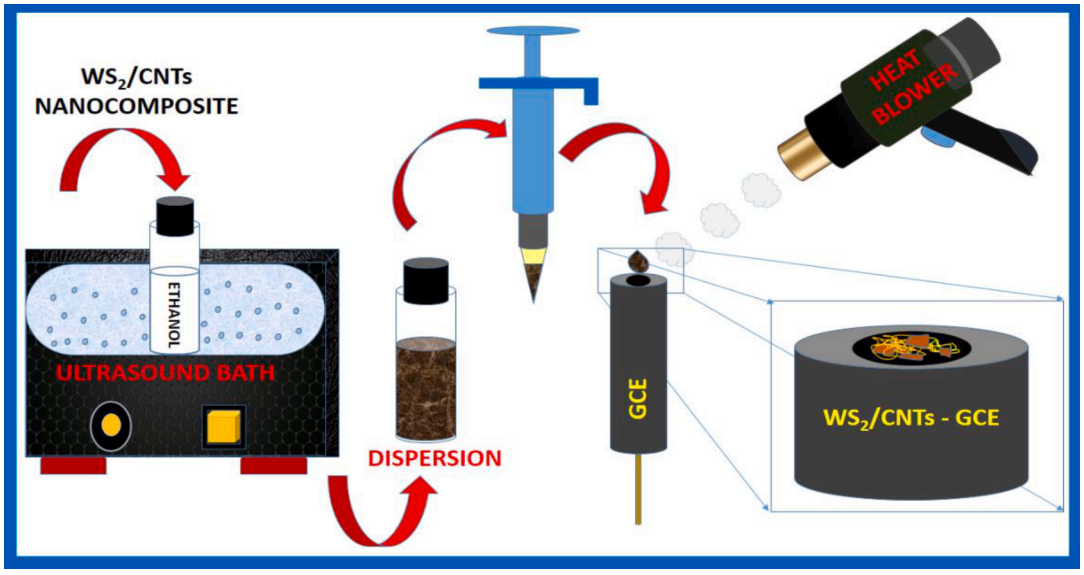

Scheme 1. WS_2/CNTs/GC modified electrode manufacturing process.

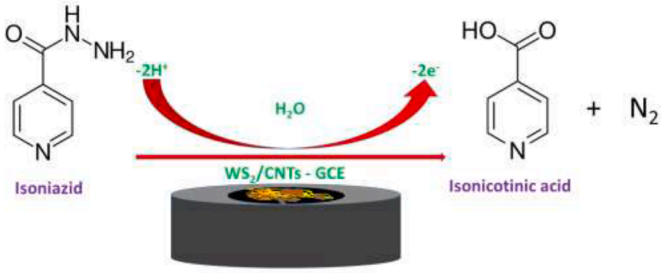

Scheme 2. Mechanism for electrochemical oxidation of isoniazid.

Table 2
Data obtained from measurement with the same modification.

$C_{isoniazid}$ (μM)	I_p (μA) 1	I_p (μA) 2	ΔI_p (μA)	Average	RSD%
10	1.00	1.05	0.05	1.02	**3.22**
20	2.36	2.30	0.05	2.33	**1.66**
30	3.64	3.53	0.12	3.58	**2.32**
40	5.14	4.87	0.26	5.00	**3.74**
50	6.21	6.25	0.04	6.23	**0.44**
60	7.60	7.35	0.25	7.47	**2.38**
70	8.63	8.46	0.17	8.54	**1.42**
80	9.75	9.66	0.08	9.71	**0.59**

Table 3
Data obtained from measurement with the different modifications.

$C_{isoniazid}$ (μM)	I_p (μA) 1	I_p (μA) 2	ΔI_p (μA)	Average	RSD%
10	1.12	0.96	0.16	1.04	**11.02**
20	2.42	2.41	0.01	2.41	**0.25**
30	3.85	3.89	0.04	3.87	**0.72**
40	5.43	5.24	0.19	5.33	**2.50**
50	7.04	6.65	0.38	6.85	**3.96**
60	8.41	8.08	0.32	8.25	**2.76**
70	9.93	9.29	0.64	9.61	**4.73**
80	10.88	10.43	0.45	10.66	**2.99**

and 5 μM). In addition, their sensor requires a more laborious manufacturing process, utilizes enzymes, which increases the cost and significantly reduces the electrode shelf life. Therefore, it is possible to conclude that the WS_2/CNT/GCE electrode manufactured in this work provides an attractive alternative to the others present in the literature regarding isoniazid sensing

Table 4
Comparison of the performance of different modified electrodes towards oxidative quantification of isoniazid.

Electrode	Technique	LOD (μM)	Linear Range (μM)	Reference
WS_2/CNT/GCE	DPV	0.24	10 - 80	This work
CoTRP(dcbpy)$_2$]-Ni/GO	BIA	3.5	100 - 1000	[1]
f-MWCNT/GCE	CV	0.27	1 - 70	[38]
MWCNT-TiO_2NPs-HRP-GCE	DPV	0.0335	0.5 - 5	[37]
Mo_2C@BMZIFs/GCE	DPV	1.5	10 - 3500	[36]
MWNT-CPE	DPV	0.5	1 - 1000	[17]
Nafion-OMC/GCE	CV/ Amperometric	0.08	0.1 - 370	[39]

The selectivity of the new electrode proposed in this work was evaluated for potential interfering species commonly present in urine. The interference produced by ammonium, sulfate, phosphate, uric acid, ascorbic acid, urea and glucose were tested by DPV. These chemical species were selected based on other studies that evaluated interferers for isoniazid [36,37,40]. The species mentioned above were assessed at two different ratios: 1:1 and 1:10 (fixed 10 μmol L^{-1} of the analyte: 10

Table 5
Selectivity study on the DPV signal of 10 μM isoniazid.

Interferents	Interfering ratio (Isoniazid:interferent)	Current signal variation (%)
NH_4^+	1:1	−5,62
	1:10	−6,70
SO_4^{2-}	1:1	−4,30
	1:10	−7,43
PO_4^{3-}	1:1	−2,22
	1:10	−8,31
Uric Acid	1:1	−5,25
	1:10	−15,25
Ascorbic Acid	1:1	−4,30
	1:10	−2,55
Glucose	1:1	−3,13
	1:10	−4,96
Ureia	1:1	−6,19
	1:10	−9,16

and 100 μmol L^{-1} interfering species). The results obtained are shown in **Table 5**. As can be seen, the proposed electrode is almost immune to interfering species. The slightly smaller current values observed in this table were attributed to the decrease of the isoniazid signal in the presence of these species. These decreases were very small and probably are the product of variations of viscosity of the medium. Ammonium, sulfate, phosphate, ascorbic acid, urea and glucose do not interfere in the detection of the analyte in all proportions. Uric acid is an interferent in a 1:10 ratio. However, the interference of this species can be bypassed using the standard addition method.

4. Conclusion

In this work, an electrochemical sensor based on a WS_2/CNT modified GC electrode for isoniazid detection has been successfully developed. The morphological and structural characterization of as-prepared WS_2/CNT composite was performed using SEM, EDS elemental mapping, XRD, and Raman spectroscopy. The electrochemical performance was evaluated by CV and DPV, where the WS_2/CNT/GCE sensor exhibited an LOD of 0.24 μM with a linear range from 10 to 80 μM for isoniazid detection. It was verified that an intense current signal originated from the oxidation of this antibiotic drug, attributed to the high conductivity/electrocatalysis proportionated by the carbon nanotubes associated with the WS_2 nanomaterial. The results of recovery experiments ranged from 96.9 to 104.5%, indicating satisfactory accuracy of the method developed. The improvement of electrochemical activity was assigned to synergic effects obtained by combining the catalytic sites from WS_2 and the known electrical conductivity and large surface area of the CNTs. This proposed electrochemical sensor has promising potential for isoniazid determination in biological samples.

Declaration of Competing Interest

The authors declare that they do not have any commercial or associative interest that represents a conflict of interest in connection with the work submitted.

Acknowledgments

The authors acknowledge the Brazilian agencies for their support: FAPESP (grant numbers: 2019/22126–2, 2018/16896–7, 2020/00325–0, 2012/50259–8 and projects 2017/13137–5 and 2014/50867–3), CNPq (grant numbers: 311847–2018–8 and project 465389/2014–7) and CAPES (CAPES-PRINT, grant number: 88887.310281/2018–00). The authors are also grateful to Central Analítica (IQ-USP) for providing chemical-analysis infrastructure. We thank Prof. Koiti Araki (Laboratório de Química Supramolecular e Nanotecnologia, IQ-USP) and SisNANO USP for the use of XRD/Raman spectroscopy facility.

References

[1] J.S. Aguirre-Araque, J.M. Gonçalves, M. Nakamura, P.O. Rossini, L. Angnes, K. Araki, et al., GO composite encompassing a tetraruthenated cobalt porphyrin-Ni coordination polymer and its behavior as isoniazid BIA sensor, Electrochim. Acta 300 (2019) 113–122, https://doi.org/10.1016/j.electacta.2019.01.097.

[2] A. Farokhi-Fard, B. Golichenari, M. Mohammadi Ghanbarlou, S. Zanganeh, F. Vaziri, Electroanalysis of isoniazid and rifampicin: Role of nanomaterial electrode modifiers, Biosens. Bioelectron. 146 (2019), 111731 https://doi.org/10.1016/j.bios.2019.111731.

[3] K.C. Chang, C.C. Leung, W.W. Yew, C.M. Tam, Standard anti-tuberculosis treatment and hepatotoxicity: Do dosing schedules matter? Eur. Respir. J. 29 (2007) 347, 10.1183/09031936.00090306.

[4] L. Qian, A.R. Thiruppathi, J. van der Zalm, A. Chen, Graphene oxide-based nanomaterials for the electrochemical sensing of isoniazid, ACS Appl. Nano Mater. 4 (2021) 3696–3706, 10.1021/acsanm.1c00178.

[5] S.-.B. He, L. Yang, X.-.L. Lin, L.-.M. Chen, H.-.P. Peng, H.-.H. Deng, et al., Heparin-platinum nanozymes with enhanced oxidase-like activity for the colorimetric sensing of isoniazid, Talanta 211 (2020), 120707 https://doi.org/10.1016/j.talanta.2019.120707.

[6] R.A.S. Lapa, J.L.F.C. Lima, J.L.M. Santos, Fluorimetric determination of isoniazid by oxidation with cerium(IV) in a multicommutated flow system, Anal. Chim. Acta 419 (2000) 17–23, doi: https://doi.org/10.1016/S0003-2670(00)00995-8.

[7] A.M. El-Brashy, S.M. El-Ashry, Colorimetric and titrimetric assay of isoniazid, J. Pharm. Biomed. Anal. 10 (1992) 421–426, doi: https://doi.org/10.1016/0731-7085(92)80060-Z.

[8] O. Hernández-González, S. Zarazúa, J.I. Veytia-Bucheli, M.M. González-Chávez, C. J. Rodríguez-Pinal, S.E. Medellín-Garibay, et al., Quantification of pyrazinamide, isoniazid, acetyl-isoniazid, and rifampicin by a high-performance liquid chromatography method in human plasma from patients with tuberculosis, J. Separ. Sci. 44 (2021) 521–529, https://doi.org/10.1002/jssc.202000672.

[9] L. Lahuerta Zamora, J.V. Garcia Mateo, J. Martinez Calatayud, Entrapment of reagents in polymeric materials. Indirect atomic absorption spectrometric determination of isoniazid by oxidation with manganese dioxide incorporated in polyester resin beads in a flow-injection system, Anal. Chim. Acta 265 (1992) 81–86, doi: https://doi.org/10.1016/0003-2670(92)85157-2.

[10] A. Wang, W. Zhang, J. Sun, J. Liu, Y. Sang, S. Gao, et al., HPLC–MS Analysis of isoniazid in dog plasma, Chromatographia 66 (2007) 741–745, 10.1365/s10337-007-0391-7.

[11] M.A. Mohammed, S.M. Abbas, J.M.S. Jamur, Derivative spectrophotometric determination for simultaneous estimation of isoniazid and ciprofloxacin in mixture and pharmaceutical formulation, Method Obj. Chem. Anal. 15 (2020) 105–110, doi: DOI: 10.17721/moca.2020.105-110.

[12] J. Wang, J. Zhao, J. Yang, J. Cheng, Y. Tan, H. Feng, et al., An electrochemical sensor based on MOF-derived NiO@ZnO hollow microspheres for isoniazid determination, Microchim. Acta 187 (2020) 380, 10.1007/s00604-020-04305-8.

[13] R. Chokkareddy, G.G. Redhi, Recent sensing technologies for first line anti-tuberculosis drugs in pharmaceutical dosages and biological fluids: A review, Sens. Lett. 17 (2019) 833–858, 10.1166/sl.2019.4157.

[14] J.M. Gonçalves, R.R. Guimarães, B.B.N.S. Brandão, L.P.H. Saravia, P.O. Rossini, C. V. Nunes, et al., Nanostructured Alpha-NiCe mixed hydroxide for highly sensitive amperometric prednisone sensors, Electrochim. Acta 247 (2017) 30–40, https://doi.org/10.1016/j.electacta.2017.06.166.

[15] C. Rajasekhar, G.R. Gan, A facile electrochemical sensor based on ionic liquid functionalized multiwalled carbon nanotubes for isoniazid detection, J. Anal. Chem. 75 (2020) 1638–1646, 10.1134/s1061934820120059.

[16] K.V. Özdokur, Voltammetric determination of isoniazid drug in various matrix by using CuOx decorated MW-CNT modified glassy carbon electrode, Electroanalysis 32 (2020) 489–495, https://doi.org/10.1002/elan.201900307.

[17] S. Shahrokhian, M. Amiri, Multi-walled carbon nanotube paste electrode for selective voltammetric detection of isoniazid, Microchim. Acta 157 (2007) 149–158, 10.1007/s00604-006-0665-z.

[18] R.F. Spindola, H. Zanin, C.S. Macena, A. Contin, R. de Cássia Silva Luz, F.S. Damos, Evaluation of a novel composite based on functionalized multiwalled carbon nanotube and iron phthalocyanine for electroanalytical determination of isoniazid, J. Solid State Electrochem. 21 (2017) 1089–1099, 10.1007/s10008-016-3451-9.

[19] P.R. Oliveira, M.M. Oliveira, A.J.G. Zarbin, L.H. Marcolino-Junior, M.F. Bergamini, Flow injection amperometric determination of isoniazid using a screen-printed carbon electrode modified with silver hexacyanoferrates nanoparticles, Sens. Actuators B 171 (172) (2012) 795–802, https://doi.org/10.1016/j.snb.2012.05.073.

[20] G. Absalan, M. Akhond, M. Soleimani, H. Ershadifar, Efficient electrocatalytic oxidation and determination of isoniazid on carbon ionic liquid electrode modified with electrodeposited palladium nanoparticles, J. Electroanal. Chem. 761 (2016) 1–7, https://doi.org/10.1016/j.jelechem.2015.11.041.

[21] R. Tenne, L. Margulis, M. Genut, G. Hodes, Polyhedral and cylindrical structures of tungsten disulphide, Nature 360 (1992) 444–446, doi:10.1038/360444a0.

[22] Xi Qiang, Zhou Dian-Ming, Kan Ying-Ya, Ge Jia, Wu Zhen-Kun, Yu Ru-Qin, Jiang Jian-Hui, Highly sensitive and selective strategy for microRNA detection based on WS_2 nanosheet mediated fluorescence quenching and duplex-specific nuclease signal amplification, Anal. Chem. 86 (2014) 1361–1365, https://doi.org/10.1021/ac403944c.

[22] Yunxia Yuan, Runqing Li, Zhihong Liu, Establishing water-soluble layered WS_2 nanosheet as a platform for biosensing, Anal. Chem. 86 (2014) 3610–3615, 2014https://doi.org/10.1021/ac5002096.

[24] Ke-Jing Huang, Yu-Jie Liu, Jun-Tao Cao, Hai-Bo Wang, An aptamer electrochemical assay for sensitive detection of immunoglobulin e based on tungsten disulfide–graphene composites and gold nanoparticles, RSC Adv. 4 (2014) 36742–36748, https://doi.org/10.1039/C4RA06133K.

[25] L.P. Silva, B.C. Lourencao, O. Fatibello-Filho, Simultaneous voltammetric determination of amlodipine besylate and hydrochlorothiazide in synthetic urine samples using a boron-doped diamond electrode, Quim. Nova, 38 (2015) 801–806, https://doi.org/10.5935/0100-4042.20150077.

[26] V. Mani, M. Govindasamy, S.-.M. Chen, R. Karthik, S.-.T. Huang, Determination of dopamine using a glassy carbon electrode modified with a graphene and carbon nanotube hybrid decorated with molybdenum disulfide flowers, Microchim. Acta 183 (2016) 2267–2275, 10.1007/s00604-016-1864-x.

[27] S. Sharma, S. Bhagat, J. Singh, R.C. Singh, S. Sharma, Excitation-dependent photoluminescence from WS_2 nanostructures synthesized via top-down approach, J. Mater. Sci. 52 (2017) 11326–11336, 10.1007/s10853-017-1303-3.

[28] S. Jana, P. Bera, B. Chakraborty, B.C. Mitra, A. Mondal, Impact of annealing on the electrodeposited WS_2 thin films: Enhanced photodegradation of coupled semiconductor, Appl. Surf. Sci. 317 (2014) 154–159, https://doi.org/10.1016/j.apsusc.2014.07.151.

[29] D. Balram, K.-.Y. Lian, N. Sebastian, N. Rasana, Surface functionalization of CNTs with amine group and decoration of begonia-like ZnO for detection of antipyretic

drug acetaminophen, Appl. Surf. Sci. 559 (2021), 149981 https://doi.org/10.1016/j.apsusc.2021.149981.
[30] M. Thripuranthaka, R.V. Kashid, C. Sekhar Rout, D.J. Late, Temperature dependent Raman spectroscopy of chemically derived few layer MoS_2 and WS_2 nanosheets, Appl. Phys. Lett. 104 (2014), 081911, 10.1063/1.4866782.
[31] X. Zhang, X.-.F. Qiao, W. Shi, J.-.B. Wu, D.-.S. Jiang, P.-.H. Tan, Phonon and Raman scattering of two-dimensional transition metal dichalcogenides from monolayer, multilayer to bulk material, Chem. Soc. Rev. 44 (2015) 2757–2785, 10.1039/c4cs00282b.
[32] Y. Wang, D. Kong, W. Shi, B. Liu, G.J. Sim, Q. Ge, et al., Ice templated free-standing hierarchically WS_2/CNT-rGO aerogel for high-performance rechargeable lithium and sodium ion batteries, Adv. Energy Mater. 6 (2016), 1601057 https://doi.org/10.1002/aenm.201601057.
[33] M. Latha, S. Biswas, J.V. Rani, Application of WS2-G composite as cathode for rechargeable magnesium batteries, Ionics 26 (2020) 3395–3404, 10.1007/s11581-020-03512-w.
[34] C.R. Rawool, A.K. Srivastava, A dual template imprinted polymer modified electrochemical sensor based on Cu metal organic framework/mesoporous carbon for highly sensitive and selective recognition of rifampicin and isoniazid, Sens. Actuators B 228 (2019) 493–506, https://doi.org/10.1016/j.snb.2019.03.032.
[35] D.P. Rocha, C.W. Foster, R.A.A. Munoz, G.A. Buller, E.M. Keefe, C.E. Banks, Trace manganese detection via differential pulse cathodic stripping voltammetry using disposable electrodes: additively manufactured nanographite electrochemical sensing platforms, Analyst 145 (2020) 3424–3430, 10.1039/d0an00018c.
[36] W. Liang, H. Ren, Y. Li, H. Qiu, B.-.C. Ye, A robust electrochemical sensing based on bimetallic metal-organic framework mediated Mo_2C for simultaneous determination of acetaminophen and isoniazid, Anal. Chim. Acta 1136 (2020) 99–105, https://doi.org/10.1016/j.aca.2020.08.044.
[37] R. Chokkareddy, N.K. Bhajanthri, G.G. Redhi, An enzyme-induced novel biosensor for the sensitive electrochemical determination of isoniazid, Biosensors 7 (2017) 1–12, 10.3390/bios7020021.
[38] W.-.C. Chen, B. Unnikrishnan, S.-.M. Chen, Electrochemical oxidation and amperometric determination of isoniazid at functionalized multiwalled carbon nanotube modified electrode, Int. J. Electrochem. Sci. 7 (2012) 9138–9149.
[39] X. Yan, X. Bo, L. Guo, Electrochemical behaviors and determination of isoniazid at ordered mesoporous carbon modified electrode, Sens. Actuators B 155 (2011) 837–842, https://doi.org/10.1016/j.snb.2011.01.058.
[40] C.R. Rawool, A.K. Srivastava, A dual template imprinted polymer modified electrochemical sensor based on Cu metal organic framework/mesoporous carbon for highly sensitive and selective recognition of rifampicin and isoniazid, Sens. Actuators B 288 (2019) 493–506, https://doi.org/10.1016/j.snb.2019.03.032.